Training-Based Spectral Reconstruction from a Single RGB Image

Rang M.H. Nguyen, Dilip K. Prasad, and Michael S. Brown

School of Computing, National University of Singapore

Abstract. This paper focuses on a training-based method to reconstruct a scene's spectral reflectance from a single RGB image captured by a camera with known spectral response. In particular, we explore a new strategy to use training images to model the mapping between camera-specific RGB values and scene reflectance spectra. Our method is based on a radial basis function network that leverages RGB white-balancing to normalize the scene illumination to recover the scene reflectance. We show that our method provides the best result against three state-of-art methods, especially when the tested illumination is not included in the training stage. In addition, we also show an effective approach to recover the spectral illumination from the reconstructed spectral reflectance and RGB image. As a part of this work, we present a newly captured, publicly available, data set of hyperspectral images that are useful for addressing problems pertaining to spectral imaging, analysis and processing.

1 Introduction

A scene visible to the human eye is composed of the scene's spectral reflectance and the scene spectral illumination which spans visible wavelengths. Commodity cameras use filters on their sensors to convert the incoming light spectra into three color channels (denoted as Red, Green, and Blue). While only three color channels are needed to reproduce the *perceptual* quality of the scene, the projective nature of the imaging process results in a loss of the spectral information.

Directly capturing spectral information from specialized hyperspectral cameras remains costly. The goal of this work is to reconstruct a scene's spectral properties, i.e. scene reflection and illumination, from a single RGB image (see Figure 1). This is done by learning a mapping between spectral responses and their corresponding RGB values for a given make and model of a camera.

Prior work in this area follow a similar training-based approach, but attempt to find a mapping using RGB images where the effects of different illumination are included in the learning process. This makes these approaches sensitive to input images captured under illuminations which were not present in the training data.

Contribution. We introduce a new strategy that learns a non-linear mapping based on a radial basis function network between the training-data and RGB images. Our approach uses a white-balance step to provide an approximate normalization of the illumination in the RGB images to improve the learned mapping

D. Fleet et al. (Eds.): ECCV 2014, Part VII, LNCS 8695, pp. 186–201, 2014.

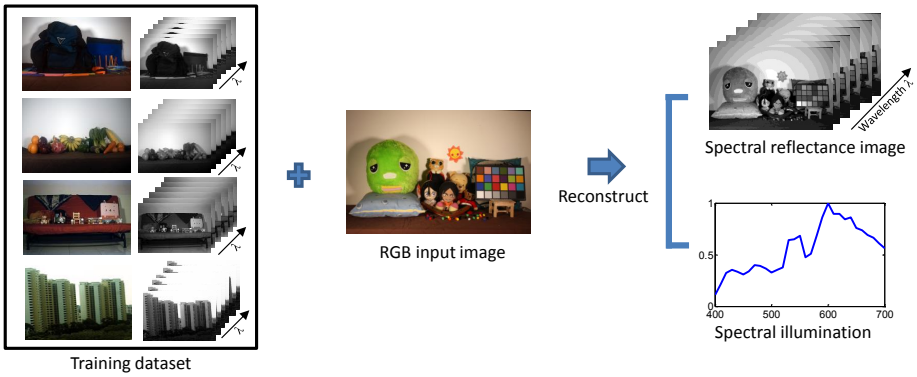

Fig. 1. Our approach takes in an input RGB image and then estimates both the spectral reflectance and the overall spectral illumination based on pre-computed training dataset

between the RGB images and spectral reflectances. This white-balance step also helps in making our approach robust to input images captured under illuminations not in our training data. Moreover, we propose a technique to estimate the illumination given our estimated spectral reflectance. Our experimental results demonstrate our approach is superior to prior methods. An additional contribution of our work is a publicly available spectral image dataset of dozens of real-world scenes taken under a number of illuminations.

2 Related Work

The need to reconstruct the spectral properties of scene reflectance (and illumination) from a three channel device or a standard color space (such as CIE-XYZ) was recognized as early as 1980s [14,15,20,21,24]. Several works targeted the reconstruction of the spectral properties of standard color samples such as the Munsell Book of Colors [2,8,10,11,15,20,24], OSA UCS [11], Swedish Natural Color System [11], and Pantone dataset [17]. Additionally, [15] considered the spectral reflectances of natural objects also.

Virtually all methods rely on the use of training-data to learn a mapping between RGB images and the corresponding spectra. For many years, a linear model was considered sufficient for this problem. It was determined using statistical analysis on standard color samples that a few (typically 3-10) basis functions are sufficient to represent the spectral reflectances [15,20,24,32]. Further, in general, basis functions were assumed to be continuous and band limited [20,24]. Most methods considered either PCA bases [2,3,11,15,17,20,30] or the Karhunen-Loeve transformation [8,10,24,25,28,32] (also called matrix R approach) which were typically pre-learnt using a few hundred to a little more than thousand spectral samples. Interestingly, [11] consider two types of PCA bases - one with least squares fit and another with assumption that the tristimulus function of

the sensor and the illumination are known. The latter approach is more accurate although it is restricted in application since illumination is generally unknown.

An interesting statistical approach was used in [22] where the bases were chosen not to minimize the error in spectral reflectance representation alone, but to minimize the error in predicting the sensor response as well such that the spectral response function of the sensor plays a role in determining the suitable bases. In the work of Abed et al. [1], a tessellation of the scatter RGB points and their reflectance spectra of a standard color chart (for a given illumination) was used as a nearest-neighbor look-up table. Then, in the general case of a scene in the same illumination, the reflectance of the nodes of the polytope that encloses the scene's RGB point are used to interpolate the reflectance at that point.

Recently, the need of non-linear mappings was recognized [4,26,29], though such a requirement was indicated earlier in [22]. Further, it was recognized by some researchers that while PCA itself may be insufficient for accurate reconstruction of spectral reflectance, splitting the color space into overlapping subspaces of 10 different hues [3,30] and low-chromaticity sub-space [30] and then using PCA on each subspace performs better. Similarly, Agahian et al. [2] proposed to put weighted coefficients for each spectral reflectance in the dataset before computing PCA. Some works [9,11] highlight that illumination has a direct and important role in the ability to reconstruct the spectral reflectances. Using Bayesian decision theory, Brainard and Freeman [5] reconstructed both spectral reflectance and illumination information for color constancy. Lenz et al. [18] statistically approximated the logarithm of the reflectance spectra of Munsell and NCS color chips instead of the usual reflectance spectra themselves. Further they computed approximate distribution of the illuminant and showed its utility for color constancy.

In our work, we consider a novel non-linear mapping strategy for modeling the mapping between camera-specific RGB values and scene reflectance spectra. Specifically, we use a radial basis function network for modeling the mapping. Our model for spectral reflectances is made illumination independent by using RGB white-balancing to normalize the scene illumination before reconstructing the spectral reflectance.

The remainder of this paper is organized as follows: Sections 3 and 4 present our approaches for spectral reflectance and illumination reconstruction, respectively; Section 5 presents the details of our spectral image dataset; Section 6 describes reconstruction results using three commercial cameras; Section 7 concludes the paper.

3 Scene Reflectance Reconstruction

As discussed in previous section, most of the methods for reconstructing reflectance are not clear how to deal with different illuminations. For example, consider we have two different spectral reflectances $R_1(\lambda)$ and $R_2(\lambda)$ illuminated by two different spectral illuminations $L_1(\lambda)$ and $L_2(\lambda)$ respectively. It is possible that under a certain observer $C_c(\lambda)$ (where $c = r, g, b$), these two

spectral reflectances share the same RGB values as described in Eq. 1. This metamer problem can be expressed as:

$$\int_{\lambda} L_1(\lambda)R_1(\lambda)C_c(\lambda)\,\mathrm{d}\lambda = \int_{\lambda} L_2(\lambda)R_2(\lambda)C_c(\lambda)\,\mathrm{d}\lambda. \tag{1}$$

From the above equation, we see it is difficult to determine whether the reflectance is $R_1(\lambda)$ or $R_2(\lambda)$ when information about illumination is not available. Therefore, one mapping for all illuminations can not handle this case. One straightforward solution is to build a mapping for each illumination. This approach will be the best in terms of reconstruction accuracy. However, it requires not only a huge effort to calibrate mappings over all illuminations but also known illumination of a new scene for reconstructing its reflectance. This approach is impractical for most applications.

In our approach, the illumination in the RGB is normalized before it is used for learning. The RGB images have been corrected using conventional white-balancing method. The details are discussed in Section 3.2. The following are four assumptions made in our approach:

- The mapping is specific to the camera and one mapping for a camera can be used for any spectral reflectance.
- The color matching functions of the camera are known.
- The scene is illuminated by a uniform illumination.
- The white balancing algorithm gives good performance for images taken under a variety of illuminations.

3.1 Pre-requisites

In this paper, we do not use RGB images taken directly from the camera. Instead, we synthesize RGB images from hyperspectral images using known camera's sensitivity functions. Computing the RGB images in this manner gives us two main advantages. Firstly, it removes the need to create a dataset of the images captured using the chosen camera for the same scenes as captured by the spectral camera. This method can be used for any commercial camera so far as its sensitivity functions are known. Note however that it is possible to use a given camera, however, care will be needed to ensure spatial scene correspondence between the RGB image and spectral image. This will likely limit the training data to planar scenes for accurate correspondence.

Color Matching Functions. The color matching functions are generally measured using sophisticated instruments. However, recent methods were proposed to reconstruct the color matching functions using standard colorcharts and illuminations satisfying certain practical requirements (for more details, see [16,27]). Alternatively, existing datasets such as [31] can be used if the chosen camera is a part of these datasets. Irrespective of the method used, measurement/estimation of the color matching functions is a one time process and the color matching functions can be stored for further use.

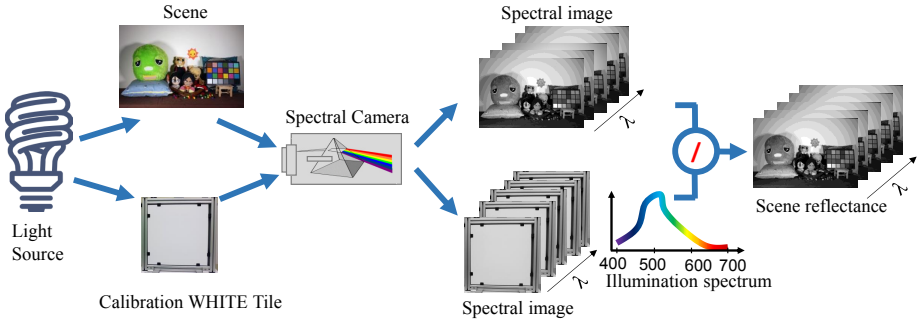

Fig. 2. This figure shows how to obtain scene reflectance and spectral illumination using a hyperspectral camera. First, a spectral image is captured from the real scene. Then, a calibration white tile is used to measure the illumination spectrum. Finally, the scene reflectance is obtained by dividing the spectral image by the illumination spectrum.

Illuminations. To obtain the illumination spectrum, we use a calibration white tile supplied with the spectral camera to capture a spectral image of the white tile illuminated by the light source (see Figure 2). We represent the spectral image captured using white tile as $S_W(\lambda, x)$, where λ is the wavelength, x is the pixel index, W denotes the white tile, and S denotes the spectral intensity captured using the spectral camera. The spectral illumination $L(\lambda)$ is computed as the average of the spectral information at all the pixels as follows:

$$L(\lambda) = \frac{1}{N} \sum_{x=1}^{N} S_W(\lambda, x) \tag{2}$$

where N is the total number of pixels.

Spectral Reflectances. After obtaining the spectral illumination, the spectral reflectance $R(\lambda, x)$ corresponding to each pixel in the spectral image $S(\lambda, x)$ can be computed directly as follows:

$$R(\lambda, x) = S(\lambda, x)/L(\lambda) \tag{3}$$

3.2 Training Stage

As discussed in the previous section, most existing methods consider computing mappings between RGB images under different illuminations and their reflectances (see Figure 3-(A)). While our approach considers a mapping between RGB images under canonical illumination (using white-balancing) and their reflectances. The training process for our model is shown in Figure 3-(B). Our approach has three steps: synthesizing the RGB image, white-balancing the RGB image, and computing the mapping.

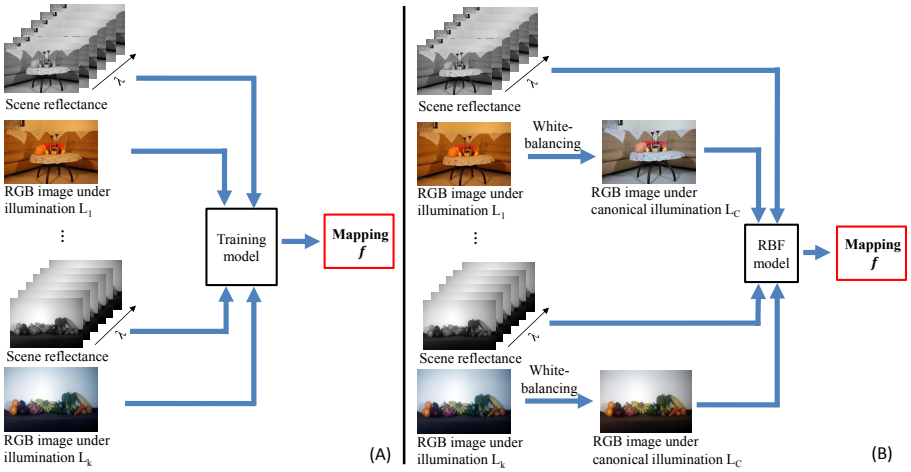

Fig. 3. This figure shows the training process for reflectance reconstruction for previous approaches and our approach. (A) shows that previous approaches consider the mapping f of RGB image to spectral reflectances. (B) shows that our approach considers the mapping f of RGB white-balanced image to the spectral reflectances.

Firstly, synthesized the RGB images corresponding to scenes and illuminations in spectral images can be formed by using the intrinsic image model as:

$$I_c(x) = \int_{\lambda} L(\lambda) R(\lambda, x) C_c(\lambda)\, \mathrm{d}\lambda \tag{4}$$

where $L(\lambda)$ is the illumination spectrum, $R(\lambda, x)$ is the scene reflectance for the pixel x, $C_c(\lambda)$ is the color matching function for the c^{th} color channel, and $c = r, g, b$ is the color channel.

After forming the RGB image $I_c(x)$, we obtain a white balanced image $\widehat{I}_c(x)$ as follows:

$$\widehat{I}_c(x) = \mathrm{diag}\left(\frac{1}{t_\mathrm{r}}, \frac{1}{t_\mathrm{g}}, \frac{1}{t_\mathrm{b}}\right) I_c(x) \tag{5}$$

where $\mathbf{t} = [t_\mathrm{r}, t_\mathrm{g}, t_\mathrm{b}]$ is the white balancing vector obtained by a chosen white balancing algorithm. For the white-balancing step, we have used shades of grey (SoG) method [12] that uses the Minkowsky norm of order 5. We note that several other methods are known for white balancing [7,13]. Here, we have chosen SoG for its simplicity, low computational requirement and proven efficacy over various datasets[1].

Next, a mapping f is learnt between the white balanced RGB images $\widehat{I}_c(x)$ and their spectral reflectances. Because we cannot guarantee the uniformity of the spectral and RGB samples, we use scatter point interpolation based on a radial basis function (RBF) network for mapping. RBF network is a popular

[1] http:/www.colorconstancy.com/

interpolation method in multidimensional space. It is used to implement a mapping $f : \mathbb{R}^3 \to \mathbb{R}^P$ according to

$$f(x) = w_0 + \sum_{i=1}^{M} w_i \phi(\|x - c_i\|) \tag{6}$$

where $x \in \mathbb{R}^3$ is the RGB input value, $f(x) \in \mathbb{R}^P$ is the spectral reflectance value in P-dimensional space, $\phi(.)$ is the radial basis function, $\|.\|$ denotes the Euclidean distance, w_i $(0 \leq i \leq M)$ are the weights, $c_i \in \mathbb{R}^3$ $(1 \leq i \leq M)$ are the RBF centers, M is the number of center. The RBF centers c_i are chosen by the orthogonal least squares method. The weights w_i are determined using linear least squares method. For more information see [6].

To control the number of centers M for the RBF network model against overfitting, we use repeated random sub-sampling validation to do cross-validation. Specifically, we randomly split the data into two sets: a training set and a validation set. The RBF network model is fitted by the training set and its generalization ability is assessed by the validation set. We ran this procedure several times on our data and found that the number of centers M which gave the best result for validation set was within $45 - 50$.

3.3 Reconstruction Stage

Once the training is performed, the mapping can be saved and used offline for spectral reflectance reconstruction. To reconstruct spectral reflectance for a new RGB image, this image must be white-balanced to transform the image to the normalized illumination space $\widehat{I}_{rgb}(x)$. The learned mapping f is used to map the white-balanced image to the spectral reflectance image as in Eq. 7.

$$R(\lambda, x) = f(\widehat{I}_{rgb}(x)) \tag{7}$$

4 Spectral Illumination Reconstruction

In theory, the spectral illumination $L(\lambda)$ can be solved from Eq. 4 when given the spectral reflectance $R(\lambda, x)$ (estimated in Section 3.3), camera sensitivity functions $C_c(\lambda)$ (given) and RGB values $I_c(x)$ (input). This equation can be written into product of matrices as follows:

$$I_{rgb} = C\text{diag}(L)R \tag{8}$$

where I_{rgb} is a matrix of $3 \times N$, C is a matrix of $3 \times P$, L is a vector of $P \times 1$, R is a matrix of $P \times N$, P is the number of spectral bands, and N is the number of pixels.

To solve the vector L, Eq. 8 needs to be rewritten as follows:

$$I = TL \tag{9}$$

where $I = [I_r, I_g, I_b]^\top$ is a vector of $3N \times 1$, $T = [\text{diag}(C_r)R, \text{diag}(C_g)R, \text{diag}(C_b)R]^\top$ is a matrix of $3N \times P$.

This means that the spectral illumination $L(\lambda)$ can be solved in a linear least squares manner. However, in practice the noise in $I_c(x)$ and the inaccuracy in estimation of $R(x, \lambda)$ impedes the reconstruction of $L(\lambda)$. As a result, it is necessary to include additional non-negative and smoothness constraints into the optimization function before solving $L(\lambda)$ as Eq. 10. This step is similar with work proposed by Park et al. [23] and can be expressed as follows:

$$\begin{aligned} L = \ & \arg\min_L \left(||TL - I||_2^2 + \alpha \, ||WL||_2^2 \right) \\ & \text{s.t } L \geq 0 \end{aligned} \tag{10}$$

where $\|.\|_2$ denotes l^2-*norm*, the term α is a weight for the smoothness constraint, and W is the first-derivative matrix defined as follows:

$$W = \begin{vmatrix} 0 & 0 & \dots & 0 & 0 \\ 1 & -1 & \dots & 0 & 0 \\ & & \dots & & \\ 0 & 0 & \dots & 1 & -1 \end{vmatrix} \tag{11}$$

We additionally use PCA basis functions to allow $L(\lambda)$ to fall in a definite subspace. Therefore, spectral illumination $L(\lambda)$ can be described as

$$L(\lambda) = \sum_{i=1}^{M} a_i B_i(\lambda) \tag{12}$$

where $B_i(\lambda)$ are the basis functions, a_i are the corresponding coefficients, and M is the number of basis functions. Eq. 12 can be rewritten into product of matrices as follows:

$$L = B\mathbf{a}$$

where $\mathbf{a} = [a_i]_{i=1}^M$ is the vector of the coefficients, and $B = [B_i]_{i=1}^M$ is the matrix of the basis functions.

Thus, the optimization function in Eq. 10 becomes:

$$\begin{aligned} \mathbf{a} = \ & \arg\min_{\mathbf{a}} \left(||TB\mathbf{a} - I||_2^2 + \alpha \, ||WB\mathbf{a}||_2^2 \right) \\ & \text{s.t } B\mathbf{a} \geq 0 \end{aligned} \tag{13}$$

Eq. 13 is a convex optimization and the global solution can be easily obtained. To make it more robust against noise from T and I (as discussed above), the optimization step in Eq. 13 should be run several times, and for each time, noise samples are removed from T and I. To determine them, the spectral illumination L is estimated and the error for each pixel is computed as in Eq. 14 at each time.

$$\epsilon(x) = \|C\text{diag}(L)R(x) - I_{rgb}(x)\|_2 \tag{14}$$

where x is the pixel in the image. The noise samples are determined by comparing with standard deviation. Then T and I are updated by removing these noise samples for the next run.

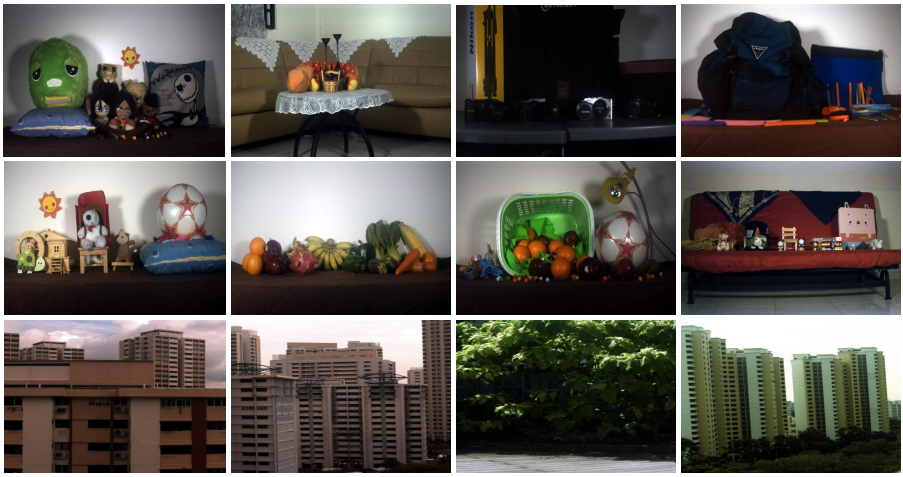

Fig. 4. This figure shows some hyperspectral images from our dataset. For visualization, these hyperspectral images are rendered to RGB images by using sensitivity functions of Canon 1D Mark III. There are a total of 64 spectral images and their corresponding illumination spectra in our dataset.

5 Dataset of Hyperspectral Images

Our dataset contains spectral images and illumination spectra taken using Specim's PFD-CL-65-V10E (400 nm to 1000 nm) spectral camera[2]. We have used an OLE23 fore lens (400 nm to 1000 nm), also from Specim. For light sources, we have considered natural sunlight and shade conditions. Additionally, we considered artificial wideband lights using metal halide lamps of different color temperatures - 2500 K, 3000 K, 3500 K, 4300K, 6500K and a commercial off-the-shelf LED E400 light. For the natural light sources, we have taken outdoor images of natural objects (plants, human beings, etc.) as well as man made objects. Further, a few images of buildings at very large focal length were also taken. The images corresponding to the other light sources have manmade objects as their scene content. For each spectral image, a total of 31 bands were used for imaging (400 nm to 700 nm at a spacing of about 10 nm). Figure 4 shows some samples from our dataset.

There are a total of 64 spectral images and their corresponding illumination spectra. We use 24 images with color charts as the test images for the reconstruction stage. This is because explicit ground truth of their spectral reflectances are available and thus the accuracy of reconstruction can be better assessed. These images are referred to as the *test images*. We have used the remaining 40 images as *training images*.

[2] `http://www.specim.fi/index.php/products/industrial/spectral-cameras/vis-vnir/`

In addition, we also used the dataset of illumination spectra from Barnard's website[3]. This dataset consists of 11 different spectral illuminations. We used these spectral illumination to synthetically generate more hyperspectral images from spectral reflectance captured by our hyperspectral camera. These hyperspectral images were used to test performance of all methods.

6 Experimental Results

In order to compare the different methods and verify their accuracy, we consider three cameras: Canon 1D Mark III, Canon 600D, and Nikon D40, whose color matching functions are available in the dataset of [31]. We first trained all methods from samples from our training images. Because the total number of pixels from 40 training images is too large and most of them are similar together, we sub-sampled each training image by using k-means clustering [19] and collected around 16,000 spectral reflectances from all the images for the training step. For the PCA method, three principal components are computed from this set of spectral reflectances. For weighted PCA proposed by Agahian et al. [2] and Delaunay interpolation proposed by Abed et al. [1], all 16,000 pairs of spectral reflectances and their corresponding RGB values are stored. Matlab code and spectral datasets used in this paper will be available online[4].

To verify the quantitative performance for the spectral reflectance reconstruction, we use two types of measurements: the goodness-of-fit coefficient (GFC) as in Eq. 15 to measure the similarity, and root mean square error (RMSE) as in Eq. 16 to measure the error.

$$s_R = \frac{1}{N} \sum_x \frac{|\sum_\lambda R(\lambda, x)\, \widehat{R}(\lambda, x)|}{\sqrt{\sum_\lambda [R(\lambda, x)]^2} \sqrt{\sum_\lambda [\widehat{R}(\lambda, x)]^2}} \tag{15}$$

$$\epsilon_R = \sqrt{\frac{\sum_x \|R(\lambda, x) - \widehat{R}(\lambda, x)\|_2^2}{N}} \tag{16}$$

where $R(x, \lambda)$ and $\widehat{R}(x, \lambda)$ are the actual and reconstructed spectral reflectances, N are the number of pixels in the image, and $\|.\|_2$ is l^2-*norm*.

We compare our method against other three methods: traditional PCA, Agahian et al. [2], and Abed et al. [1] method. Firstly, the RGB test images for reconstruction are formed using the intrinsic image model in Eq. 4. We reconstruct reflectances of 24 images (size of 1312×1924). The average time to reconstruct the whole image required by the four methods are presented in Table 1. We also test our method without using white-balance step to analyze the contribution of each steps in our framework.

[3] `http://www.cs.sfu.ca/~colour/data/colour_constancy_synthetic_test_data/index.html`

[4] `http://www.comp.nus.edu.sg/~whitebal/spectral_reconstruction/index.html`

In order to investigate the impact of illumination on the reconstruction performance, we test all the five methods on two test conditions. The first test condition considers images taken under illuminations that were *present* in the training images also. Table 2 shows the similarity and error measurement respectively under illumination *present* in training data. The second test condition considers images taken under illuminations that were *not* present in the training images. Table 3 shows the similarity and error measurement respectively under illumination *not* present in training data. The results show that our method provides the best result for spectral reflectance reconstruction in terms of both similarity and error for both test conditions. It is clear that white-balance step is important especially when the illumination is not present in training data. Moreover, RBF has better performance than other technique and much more compact than Delaunay interpolation and weighted PCA.

Table 1. This table shows the *average* time for each method to reconstruct spectral reflectances from a whole image of size 1312×1924

Methods	PCA	Agahian [2]	Abed [1]	Our
Time (s)	1.14	144.30	23.14	8.56

In addition, we also compare the actual reconstruction results for eight color patches in the color chart in Figure 5 for Canon 1D Mark III. The images are taken under indoor illumination using metal halide lamp of 4300K color temperature (spectrum in Figure 6). The ground truth of the spectral reflectances are obtained from the hyperspectral camera. The quantitative results of these patches for all methods are shown in Table 4. Again, it can be seen that our method performs better than the others methods. *Additional results are shown in the supplementary material.*

Our method also obtains good results for recovering spectral illumination. The reconstructed spectra of six illuminations are also shown in Figure 6 along with the ground truth ones. Three top illuminations are metal halide lamp 2500K, metal halide lamp 4300K and sunlight from our dataset. Three bottom illuminations are Sylvania 50MR16Q, Solux 3500K and Solux 4700K from Barnard's website. Our accuracies of the recovered spectral illumination are within $0.94 - 0.99$ in term of similarity measurement (goodness-of-fit coefficient).

We also test our method in terms of RGB accuracy. The reconstructed spectral reflectance and illumination are projected back onto the same camera sensitivity functions to measure the error in RGB space. Table 5 shows the mean values of similarity measurements s_R and error measurement ϵ_R. Our result is almost the same with the input RGB with only small errors. In addition, Figure 7 show an example of relighting application for our work. Our relit image is close to the ground truth image captured under the target illumination.

Table 2. This table shows the reflectance reconstruction results of three commercial cameras: Canon 1D Mark III, Canon 600D, and Nikon D40. he mean values of similarity measurements s_R in Eq. 15 and error measurement ϵ_R in Eq. 16 are shown. In this experiment, we test all five methods under illuminations *present* in the training data.

	Canon 1D Mark III		Canon 600D		Nikon D40	
	s_R	ϵ_R	s_R	ϵ_R	s_R	ϵ_R
PCA	0.8422	0.0957	0.8340	0.0966	0.8438	0.0947
Agahian [2]	0.8743	0.1139	0.8757	0.1079	0.8837	0.1008
Abed [1]	0.9715	0.0350	0.9707	0.0356	0.9723	0.0347
Ours w/o WB	0.9736	0.0315	0.9742	0.0313	0.9743	0.0320
Ours	**0.9802**	**0.0311**	**0.9811**	**0.0312**	**0.9805**	**0.0313**

Table 3. This table shows the reflectance reconstruction results of three commercial cameras: Canon 1D Mark III, Canon 600D, and Nikon D40. he mean values of similarity measurements s_R in Eq. 15 and error measurement ϵ_R in Eq. 16 are shown. In this experiment, we test all five methods under illuminations *not* present in the training data. These spectral illuminations are downloaded from the dataset in Barnard's website.

	Canon 1D Mark III		Canon 600D		Nikon D40	
	s_R	ϵ_R	s_R	ϵ_R	s_R	ϵ_R
PCA	0.8528	0.0873	0.8438	0.0896	0.8568	0.0856
Agahian [2]	0.8971	0.0791	0.8941	0.0793	0.8973	0.0773
Abed [1]	0.9293	0.0796	0.9107	0.0867	0.9281	0.0815
Ours w/o WB	0.9529	0.0722	0.9393	0.0727	0.9434	0.0702
Ours	**0.9805**	**0.0315**	**0.9812**	**0.0315**	**0.9810**	**0.0314**

Table 4. This table shows the reconstruction result (in RMSE) of colorchecker's reflectance using Canon 1D Mark III under indoor illumination using metal halide lamp of 4300K color temperature

	(a)	(b)	(c)	(d)	(e)	(f)	(g)	(h)
PCA	0.0464	0.0517	0.0360	0.0321	0.0597	0.0560	0.0366	0.0668
Agahian [2]	0.0470	0.0286	0.0328	0.0252	0.0511	0.0457	0.0350	0.0832
Abed [1]	0.0465	0.0845	0.0382	0.0225	0.0908	0.0507	0.0603	0.0721
Ours w/o WB	0.0367	0.0516	0.0553	0.0330	0.0474	0.0375	0.0723	**0.0292**
Ours	**0.0228**	**0.0260**	**0.0210**	**0.0117**	**0.0229**	**0.0226**	**0.0271**	0.0416

Table 5. This table shows colorimetric accuracy of our spectral reconstruction for three commercial cameras: Canon 1D Mark III, Canon 600D, and Nikon D40. The mean values of similarity measurements s_R in Eq. 15 and error measurement ϵ_R in Eq. 16 are shown.

Canon 1D Mark III		Canon 600D		Nikon D40	
s_R	ϵ_R	s_R	ϵ_R	s_R	ϵ_R
0.9967	0.0146	0.9969	0.0139	0.9929	0.0169

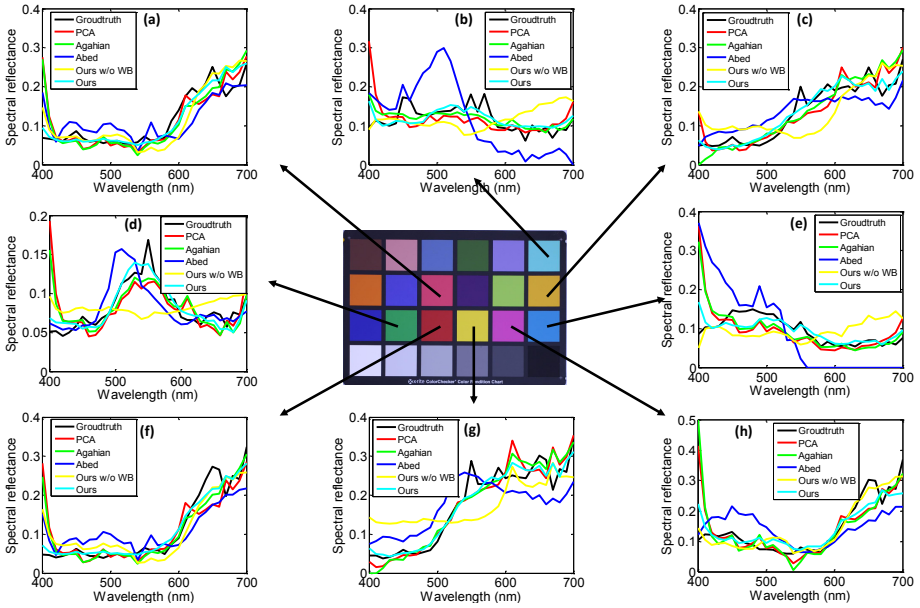

Fig. 5. This figure shows the reconstruction result of colorchecker's reflectance using Canon 1D Mark III under indoor illumination using metal halide lamp of 4300K color temperature. The quantitative errors of all patches are shown in Table 4.

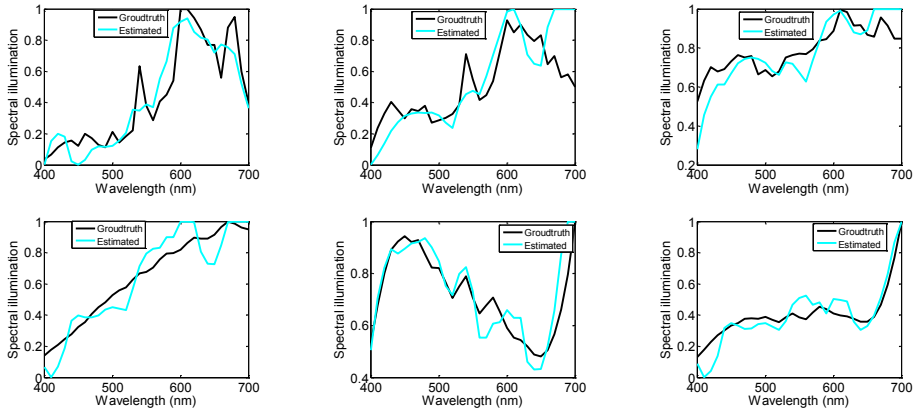

Fig. 6. This figure shows the reconstruction result for six illuminations. Three top illuminations are metal halide lamp 2500K, metal halide lamp 4300K and sunlight from our dataset. Three bottom illuminations are Sylvania 50MR16Q, Solux 3500K and Solux 4700K from Barnard's website.

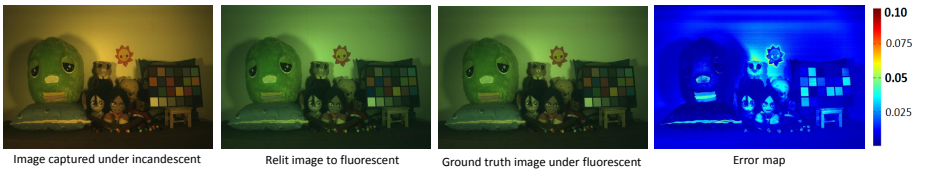

Fig. 7. This figure shows an example of relighting application

7 Discussion and Concluding Remarks

We have presented a new approach to reconstruct a spectral reflectance image from a single RGB image which is useful for several computer vision tasks, e.g. to relight the scene with a new illumination or to obtain the image under a new observer (camera). Our approach is based on a radial basis function network using white-balancing as an intermediate step. Despite the mathematical loss of the spectral data in a RGB camera, we show that the spectral reflectance can be reconstructed with low RMSE errors and high goodness-of-fit coefficients. Our method improved reconstruction performance compared with previous works, especially when the tested illumination is not included in the training data. This indicates that our method is not severely dependent on the availability of illumination information directly or indirectly. This is a result of using RGB white balancing which indirectly normalizes the illumination component in the image.

In addition, we have also proposed an effective method to recover the spectral illumination from a single RGB image and its scene's spectral reflectance (estimated from previous step). As part of this work, we have generated a much needed set of hyperspectral images that is suitable for exploring this research as well as other aspects of spectral imaging, analysis, and processing.

A limitation of our work is the assumption that a scene is illuminated by an uniform illumination. For many scene this is not the case. Moreover, although our approach can handle well the reflectance and illumination which have smooth spectra, our approach like other approaches still has poor results in case of spiky spectra. Spectral reconstruction under very narrow band illuminations or severely spiky illuminations will be interesting and challenging areas for future investigation. Another interesting areas to explore in the future will be intrinsic video and retinal imaging (where some retinal tissues can be fluorescent).

Acknowledgement. This study was funded by A*STAR grant no. 1121202020. We sincerely thank Mr. Looi Wenhe (Russell) for his help in capturing spectral images of our dataset.

References

1. Abed, F.M., Amirshahi, S.H., Abed, M.R.M.: Reconstruction of reflectance data using an interpolation technique. J. Opt. Soc. Am. A 26(3), 613–624 (2009)
2. Agahian, F., Amirshahi, S.A., Amirshahi, S.H.: Reconstruction of reflectance spectra using weighted principal component analysis. Color Research & Application 33(5), 360–371 (2008)
3. Ayala, F., Echávarri, J.F., Renet, P., Negueruela, A.I.: Use of three tristimulus values from surface reflectance spectra to calculate the principal components for reconstructing these spectra by using only three eigenvectors. J. Opt. Soc. Am. A 23(8), 2020–2026 (2006)
4. Barakzehi, M., Amirshahi, S.H., Peyvandi, S., Afjeh, M.G.: Reconstruction of total radiance spectra of fluorescent samples by means of nonlinear principal component analysis. J. Opt. Soc. Am. A 30(9), 1862–1870 (2013)
5. Brainard, D.H., Freeman, W.T.: Bayesian color constancy. J. Opt. Soc. Am. A 14(7), 1393–1411 (1997)
6. Chen, S., Cowan, C.F., Grant, P.M.: Orthogonal least squares learning algorithm for radial basis function networks. IEEE Transactions on Neural Networks 2(2), 302–309 (1991)
7. Cheng, D., Prasad, D.K., Brown, M.S.: Illuminant estimation for color constancy: why spatial-domain methods work and the role of the color distribution. J. Opt. Soc. Am. A 31(5), 1049–1058 (2014)
8. Cohen, J.: Dependency of the spectral reflectance curves of the munsell color chips. Psychonomic Science (1964)
9. Connah, D., Westland, S., Thomson, M.G.: Recovering spectral information using digital camera systems. Coloration Technology 117(6), 309–312 (2001)
10. Eslahi, N., Amirshahi, S.H., Agahian, F.: Recovery of spectral data using weighted canonical correlation regression. Optical Review 16(3), 296–303 (2009)
11. Fairman, H.S., Brill, M.H.: The principal components of reflectances. Color Research & Application 29(2), 104–110 (2004)
12. Finlayson, G.D., Trezzi, E.: Shades of gray and colour constancy. In: Color and Imaging Conference, vol. 2004, pp. 37–41 (2004)
13. Gijsenij, A., Gevers, T., van de Weijer, J.: Computational color constancy: Survey and experiments. IEEE Transactions on Image Processing 20(9), 2475–2489 (2011)
14. Hall, R., Hall, R.: Illumination and color in computer generated imagery, vol. 7. Springer, New York (1989)
15. Jaaskelainen, T., Parkkinen, J., Toyooka, S.: Vector-subspace model for color representation. J. Opt. Soc. Am. A 7(4), 725–730 (1990)
16. Jiang, J., Liu, D., Gu, J., Susstrunk, S.: What is the space of spectral sensitivity functions for digital color cameras? In: IEEE Workshop on Applications of Computer Vision, pp. 168–179 (2013)
17. Laamanen, H., Jetsu, T., Jaaskelainen, T., Parkkinen, J.: Weighted compression of spectral color information. J. Opt. Soc. Am. A 25(6), 1383–1388 (2008)
18. Lenz, R., Meer, P., Hauta-Kasari, M.: Spectral-based illumination estimation and color correction. Color Research & Application 24, 98–111 (1999)
19. MacQueen, J.: Some methods for classification and analysis of multivariate observations. In: Proceedings of the fifth Berkeley Symposium on Mathematical Statistics and Probability, California, USA, vol. 1, pp. 281–297 (1967)
20. Maloney, L.T.: Evaluation of linear models of surface spectral reflectance with small numbers of parameters. J. Opt. Soc. Am. A 3(10), 1673–1683 (1986)

21. Maloney, L.T., Wandell, B.A.: Color constancy: a method for recovering surface spectral reflectance. J. Opt. Soc. Am. A 3(1), 29–33 (1986)
22. Marimont, D.H., Wandell, B.A.: Linear models of surface and illuminant spectra. J. Opt. Soc. Am. A 9(11), 1905–1913 (1992)
23. Park, J.I., Lee, M.H., Grossberg, M.D., Nayar, S.K.: Multispectral imaging using multiplexed illumination. In: International Conference on Computer Vision, pp. 1–8 (2007)
24. Parkkinen, J.P., Hallikainen, J., Jaaskelainen, T.: Characteristic spectra of munsell colors. J. Opt. Soc. Am. A 6(2), 318–322 (1989)
25. Peyvandi, S., Amirshahi, S.H.: Generalized spectral decomposition: a theory and practice to spectral reconstruction. J. Opt. Soc. Am. A 28(8), 1545–1553 (2011)
26. Peyvandi, S., Amirshahi, S.H., Hernández-Andrés, J., Nieves, J.L., Romero, J.: Spectral recovery of outdoor illumination by an extension of the bayesian inverse approach to the gaussian mixture model. J. Opt. Soc. Am. A 29(10), 2181–2189 (2012)
27. Prasad, D.K., Nguyen, R., Brown, M.S.: Quick approximation of camera's spectral response from casual lighting. In: IEEE International Conference on Computer Vision Workshops, pp. 844–851 (2013)
28. Romero, J., Garcia-Beltran, A., Hernández-Andrés, J.: Linear bases for representation of natural and artificial illuminants. J. Opt. Soc. Am. A 14(5), 1007–1014 (1997)
29. Sharma, G., Wang, S.: Spectrum recovery from colorimetric data for color reproductions. In: Color Imaging: Device-Independent Color, Color Hardcopy, and Applications VII. Proc. SPIE, vol. 4663, pp. 8–14 (2002)
30. Zhang, X., Xu, H.: Reconstructing spectral reflectance by dividing spectral space and extending the principal components in principal component analysis. J. Opt. Soc. Am. A 25(2), 371–378 (2008)
31. Zhao, H., Kawakami, R., Tan, R.T., Ikeuchi, K.: Estimating basis functions for spectral sensitivity of digital cameras. In: Meeting on Image Recognition and Understanding, vol. 1 (2009)
32. Zhao, Y., Berns, R.S.: Image-based spectral reflectance reconstruction using the matrix r method. Color Research & Application 32(5), 343–351 (2007)